Geophysical Research Letters

RESEARCH LETTER
10.1029/2021GL093814

Key Points:

- Over May to October in 2014–2017, 10 and 5 ozone pollution episodes (OPEs) occurred in North China and Yangtze River Delta, respectively
- Enhanced BVOC emissions and reduced stomatal O_3 uptakes contributed 1.4 ppbv (8.4%) and 3.8 ppbv (22.9%) O_3 to OPEs in North China and YRD
- The O_3 vegetation damages lead to positive feedbacks onto seasonal-mean surface O_3, but the feedbacks are not exacerbated during OPEs

Supporting Information:

Supporting Information may be found in the online version of this article.

Correspondence to:

H. Liao and X. Yue,
hongliao@nuist.edu.cn;
yuexu@nuist.edu.cn

Citation:

Gong, C., Liao, H., Yue, X., Ma, Y., & Lei, Y. (2021). Impacts of ozone-vegetation interactions on ozone pollution episodes in North China and the Yangtze River Delta. *Geophysical Research Letters*, *48*, e2021GL093814. https://doi.org/10.1029/2021GL093814

Received 10 APR 2021
Accepted 25 MAY 2021

Impacts of Ozone-Vegetation Interactions on Ozone Pollution Episodes in North China and the Yangtze River Delta

Cheng Gong[1,2], Hong Liao[3], Xu Yue[3], Yimian Ma[2,4], and Yadong Lei[2,4]

[1]State Key Laboratory of Atmospheric Boundary Layer Physics and Atmospheric Chemistry, Institute of Atmospheric Physics, Chinese Academy of Sciences, Beijing, China, [2]University of Chinese Academy of Sciences, Beijing, China, [3]Jiangsu Key Laboratory of Atmospheric Environment Monitoring and Pollution Control, Jiangsu Collaborative Innovation Center of Atmospheric Environment and Equipment Technology, School of Environmental Science and Engineering, Nanjing University of Information Science and Technology, Nanjing, China, [4]Climate Change Research Center, Institute of Atmospheric Physics, Chinese Academy of Sciences, Beijing, China

Abstract Persistent ozone (O_3) pollution episodes (OPEs, with regionally averaged maximum daily 8-h average (MDA8) O_3 concentration exceeding 80 ppbv and lasting for 5 days or longer) occurred frequently in megalopolis over eastern China in recent years. Here, we apply a newly developed chemistry-biosphere model (GEOS-Chem-YIBs) to comprehensively quantify the vegetation contributions to OPEs in North China and Yangtze River Delta (YRD) over May to October in 2014–2017. The simulated MDA8 O_3 concentrations increases 16.7 and 16.6 ppbv) during OPEs in North China and YRD, of which about 1.4 ppbv (8.4%) and 3.8 ppbv (22.9%) are caused by the processes including increased BVOC emissions and reduced stomatal dry deposition. Furthermore, the O_3 damages to vegetation stomata slightly increase seasonal-mean O_3 concentrations by <1 ppbv, but such effects are not exacerbated during OPEs despite the high O_3 exposure.

Plain Language Summary The summertime ozone (O_3) in eastern China has kept increasing in recent years, accompanying with more frequent persistent O_3 pollution episodes (OPEs) in North China Plain and Yangtze River Delta (YRD). Vegetation-related processes, including biogenic volatile organic compounds emissions and stomatal O_3 uptakes, significantly influence O_3 concentrations and dynamically vary with meteorology. Warm and dry weather conditions during OPEs can lead vegetation emitting more biogenic volatile organic compounds and uptaking less O_3, but the magnitudes of vegetation contributions to recent OPEs over China have not been quantified yet. Here, 10 and 5 OPEs in North China and YRD are identified over 2014–2017, respectively, which lasted for 5 or longer days with regionally averaged maximum daily 8-h average O_3 concentrations larger than 80 ppbv. By applying a newly developed chemistry-biosphere coupled model, we quantified that about 1.4 ppbv (8.4%) and 3.8 ppbv (22.9%) of simulated O_3 enhancements (16.7 and 16.6 ppbv) during OPEs were caused by vegetation-related processes in North China and YRD. Meanwhile, the O_3 damages to vegetation stomata led to positive feedbacks onto seasonal-mean surface O_3, but the feedbacks are not exacerbated during OPEs. Our results highlight the important contributions of vegetation to OPEs in eastern China.

1. Introduction

Ground-level ozone (O_3) is a secondary gas pollutant generated by photochemical reactions of nitrogen oxides (NO_x) and volatile organic compounds (VOCs) (Atkinson, 2000; Sillman, 1999), detrimental to both human health (Dang & Liao, 2019; Lelieveld et al., 2015; Lu et al., 2020) and ecosystem productions (Fuhrer et al., 1997; Lombardozzi et al., 2012; Yue et al., 2017). Since 2013, strict clean-air actions were implemented in China to alleviate the severe particulate pollution (Zheng et al., 2018) but bring little benefits to O_3 control (Li et al., 2019). With the increasing O_3 loading over China (Liu & Wang, 2020a, 2020b; Lu et al., 2018), the regional O_3 pollution episodes (OPEs, defined in this work as episodes that last for 5 days or longer and during which the regionally averaged maximum daily 8-h average (MDA8) O_3 concentrations exceed 80 ppbv) showed increases in frequency and persistence (Gong & Liao, 2019; Gong et al., 2020b). However, alleviation of O_3 pollution remains a challenge considering the nonlinear effects of NO_x-VOCs reactions

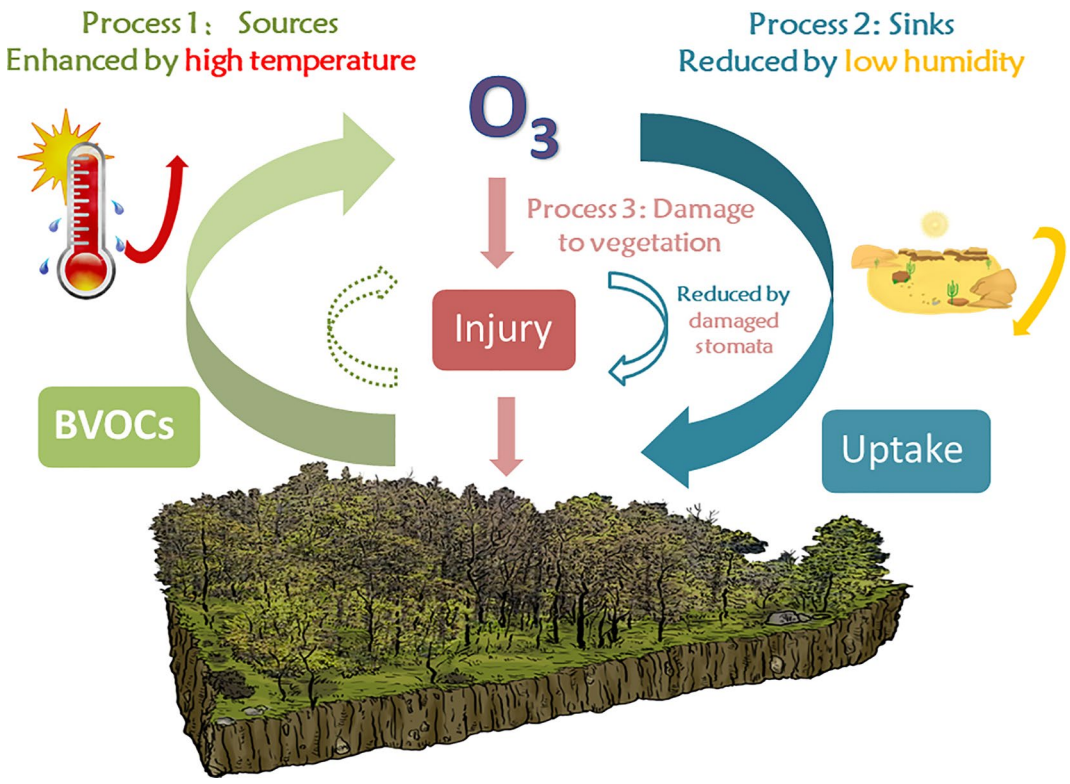

Figure 1. Summary of the vegetation processes contributing to surface O_3. Process one indicates the BVOCs emissions by vegetation, which is enhanced during OPEs by warm weather; Process two indicates the stomatal O_3 uptakes (important parts in O_3 dry deposition), which is reduced during OPEs due to the dry condition. Process three indicates the O_3 vegetation damages, which would lead feedbacks on surface O_3 by influencing Process 1 (left dashed-line arrow, not considered in this study due to the large uncertainties) and Process 2 (right hollow arrow). VOC, volatile organic compounds; BVOCs, biogenic VOCs; OPEs, ozone pollution episodes.

(Wang et al., 2019, 2017) and the significant contributions from natural sources (Lu et al., 2019; Wang et al., 2011).

Terrestrial vegetation acts as both sources and sinks of surface O_3. On one hand, biogenic VOCs (BVOCs) emitted by vegetation, such as isoprene and terpenes, are important precursors of O_3 (Calfapietra et al., 2013) (Process one in Figure 1). A recent study estimated that BVOCs emissions contributed about 15 ppbv to the MDA8 O_3 concentrations in eastern China over July-August in 2016–2017 (Lu et al., 2019). On the other hand, the stomatal O_3 uptake by vegetation (Process 2 in Figure 1) is a major process for surface O_3 removal, which contributes about 40–60% on average to the global O_3 dry deposition (Fowler et al., 2009). However, current atmospheric chemistry models mostly parameterize O_3 stomatal deposition as a function of air temperature and water vapor (Wesely & Hicks, 2000) in default, although several recent studies tried to connect O_3 dry deposition velocity (V_{d,O_3}) dynamically to vegetation biophysics in CMAQ (Emberson et al., 2013; Huang et al., 2016), CESM coupling Community Land Model (CLM) (Sadiq et al., 2017; Val Martin et al., 2014) or GFDL-AM4-LM4.0 model (Lin et al., 2020).

The O_3 injury to vegetation (Process three in Figure 1), through impairing photosynthetic enzyme activities (Ainsworth et al., 2012; Wittig et al., 2007), reducing stomatal conductance (Lombardozzi et al., 2012) and injuring vegetation leaf area index (LAI) (Feng et al., 2019a; Yue & Unger, 2014), influences both BVOCs emissions (Process one in Figure 1) and O_3 stomatal dry deposition (Process two in Figure 1) and hence results in a feedback onto O_3 level. Previous studies showed that the O_3 damage to photosynthesis and stomata reduces the stomatal dry deposition (the right hollow arrow in Figure 1) and enhances summertime-mean surface O_3 concentrations by as high as 5–6 ppbv (Clifton et al., 2020; Gong et al., 2020a; Sadiq et al., 2017). However, the effects of O_3 exposure on BVOC emissions (the left dashed-line arrow in Figure 1) remain highly uncertain. Observations showed that BVOC emissions could increase under high and

acute O_3 concentrations (Fares et al., 2010; Velikova et al., 2008) but decrease with long-term O_3 exposure (Feng et al., 2019b; Wang et al., 2020; Yuan et al., 2017). Current vegetation models generally lack proper parameterization schemes to describe such effects. Gong et al. (2020a) considered the impact of O_3 damage to vegetation on isoprene emissions in a fully coupled carbon-chemistry-climate model and found a small feedback onto simulated O_3 concentration. Therefore, the impact of vegetation damage by O_3 on BVOC emissions is not considered in this study.

OPEs tend to occur under hot and dry weather conditions (Gong & Liao, 2019; Liu et al., 2019; Pu et al., 2017; Zhang & Wang, 2016), which not only accelerate photochemical reactions (Jacob & Winner, 2009; Pusede et al., 2015) but also stimulate vegetation to emit more BVOCs (enhancing Process one in Figure 1) (Ma et al., 2019) and to close stomata (weakening process two in Figure 1) (Lin et al., 2020; Porter & Heald, 2019). Nevertheless, how changes in emissions of BVOCs (Process 1) and dry deposition of O_3 (Process 2) would alter O_3 concentrations during OPEs relative to the seasonal mean remain unclear. In addition, whether the O_3 damages to vegetation (Process 3) would be amplified and the resulted influence on O_3 concentration by altering dry deposition during severe OPEs needs to be examined.

During the warm seasons (May-October) in 2014–2017, North China (36°N–40.5°N, 114.5°E–119.5°E) and Yangtze River Delta (YRD) (29°N–33°N, 118°E–122°E) region were the most polluted regions by O_3 in China (Figure S1). Meanwhile, O_3 exposure during severe OPEs in these two regions with dense population is an urgent threat to public health (Chen et al., 2021; Kuerban et al., 2020; Liao et al., 2017). Following our definition of OPEs (Gong et al., 2020b), 10 and 5 OPEs occurred over North China and YRD, respectively (Table S1). We simulate O_3 concentrations over 2014–2017 by using the updated 3-D chemical transport model GEOS-Chem coupled with the Yale Interactive terrestrial Biosphere model (GC-YIBs) (Lei et al., 2020) with fine resolution (0.5° latitude × 0.625° longitude) over Asia (11°S–55°N, 60°E–150°E). We aim to comprehensively quantify (1) the contributions of Processes 1 and 2 to O_3 concentrations during OPEs relative to the seasonal mean; (2) the differences in O_3 concentrations with and without the O_3 damage to photosynthesis and stomatal conductance for both seasonal mean and OPEs.

2. Materials and Methods

2.1. Observed O_3 Concentrations

Ground-based hourly O_3 concentrations observed over May-October in 2014–2017 were obtained from the observational network of the China Ministry of Ecology and Environment (http://datacenter.mee.gov.cn/). Among more than 1,500 national sites, 717 with reasonable temporal coverage were selected (Figure S1) to calculate MDA8 O_3 concentrations. The criteria were as follow: (1) At least 6-h valid observations were required for the calculation of daily MDA8 O_3 concentration; (2) More than 15 days had valid MDA8 O_3 values in each month for individual site.

2.2. GC-YIBs Model

GEOS-Chem model employs a fully coupled NO_x-O_x-hydrocarbon-aerosol chemistry mechanism to simulate concentrations of gas-phase pollutants and aerosols at 47 vertical layers up to 0.1 hPa (Bey et al., 2001; Park et al., 2003; Pye et al., 2009). Photolysis rates are computed by Fast-JX scheme (Bian & Prather, 2002). Dry deposition for gases and aerosols is diagnosed based on the resistance-in-series scheme (Wesely, 1989) in the base version. BVOC emissions employ the MEGAN v2.1 biogenic emissions inventory with updates from Guenther et al. (2012). Following Dang et al. (2021), the global anthropogenic emissions inventory is from Community Emissions Data System (CEDS), while the latest Multiresolution Emission Inventory (MEIC, http://www.meicmodel.org) (Zheng et al., 2018) over 2014–2017 is used in China and the MIX inventory (Li et al., 2017) is used in the rest regions of Asia.

YIBs model is a terrestrial vegetation model including nine plant functional types (PFTs) that can simulate biophysical process (such as photosynthesis, transpiration, and respiration) and dynamically predict LAI and tree height. Leaf-level photosynthesis is calculated by Farquhar and Ball-Berry models schemes (Ball et al., 1987; Farquhar et al., 1980). Semimechanistic O_3 damage scheme (Sitch et al., 2007) is used to quantify O_3 vegetation damage, which is dependent on stomatal O_3 uptake among different PFTs (Yue

Table 1
Summary of the Model Experiments in This Study

Name	BVOCs emissions	V_{d,O_3}	O_3 damages to vegetation
	Continuous simulations over May to October in 2014–2017		
EX_GC	MEGAN	W89[a]	None
EX_GC-YIBs	MEGAN	W89[a]+Dynamic YIBs[b]	None
EX_GC-YIBs-damage	MEGAN	W89[a]+Dynamic YIBs[b]	Sitch et al. [2007] scheme
	Simulations from 1 day before to the end of OPEs		
CASE_BVOCs-fixed-NC	Fixed[c]	W89[a]+Dynamic YIBs[b]	None
CASE_BVOCs-fixed-YRD	Fixed[c]	W89[a]+Dynamic YIBs[b]	None
CASE_Vd-fixed-NC	MEGAN	Fixed[c]	None
CASE_Vd-fixed-YRD	MEGAN	Fixed[c]	None

[a]W89 indicates the Wesely (1989) dry deposition scheme. [b]Dynamic YIBs scheme is the same as W89 except dynamically updating the leaf area index and stomatal conductance from the YIBs model. [c]The BVOCs emissions or V_{d,O_3} values are fixed in the seasonal-mean values from EX_GC-YIBs during each OPE.

& Unger, 2015). In Sitch et al. (2007) scheme, there are two sets of parameters representing high and low sensitivities of vegetation to O_3 damages. Here we utilize parameters with high O_3 sensitivity to assess the maximum potential feedback of O_3-vegetation interactions.

GC-YIBs is a newly developed chemistry-biosphere model (Lei et al., 2020) driven by version two of Modern Era Retrospective-analysis for Research and Application (MERRA2) assimilated meteorological data (Molod et al., 2015). For the coupling of GC-YIBs, while the GEOS-Chem model provides simulated O_3 concentrations at each time step to drive YIBs model, YIBs updates LAI and stomatal conductance for GEOS-Chem to calculate O_3 stomatal dry deposition dynamically. Simulated gross primary productivity (GPP), LAI, and O_3 dry deposition velocity from the GC-YIBs model have been evaluated in Lei et al. (2020). Here, we extended the global version of GC-YIBs with resolution of 4° latitude × 5° longitude to the nested version with resolution of 0.5° latitude × 0.625° longitude over Asia (11°S–55°N, 60°E–150°E), whose boundary conditions are provided by global simulations at a 2° latitude × 2.5° longitude horizontal resolution. The satellite-based land types and cover fraction are aggregated into the nine PFTs and replace the Olson et al. (2001) land cover map in GEOS-Chem (Figure S2).

2.3. Sensitivity Experiments

We first performed two simulations over May to October in 2014–2017 with GEOS-Chem (named EX_GC) and GC-YIBs (named EX_GC-YIBs) models without O_3 damage to vegetation to evaluate the performance of nested GC-YIBs with fine resolution of 0.5° × 0.625°. Then the O_3 damage effects on vegetation were turned on in GC-YIBs model (named EX_GC-YIBs-damage) to quantify the differences in O_3 concentrations with and without O_3 vegetation damages. All three experiments were spin up for 5 months in each year.

In addition, four sensitivity experiments were performed to isolate the differences in O_3 concentration resulted from the changes in BVOC emissions and O_3 dry deposition velocity (V_{d,O_3}) during OPEs relative to the seasonal mean. These runs started from one day before each of the OPEs to the final day of the episode with the same configurations as EX_GC-YIBs, except that BVOC emissions (CASE_BVOCs-fixed-NC, CASE_BVOCs-fixed-YRD) or V_{d,O_3} (CASE_Vd-fixed-NC, and CASE_Vd-fixed-YRD) were fixed to the seasonal mean (May-October) values (seasonal-mean values were taken from EX_GC-YIBs simulation). The differences in MDA8 O_3 concentrations between EX_GC-YIBs simulation and these sensitivity experiments are used to diagnose the role of O_3-vegetation interactions in the enhancements of O_3 during OPEs. BVOCs species from MEGAN that are used in GC-YIBs are shown in Table S2. All experiments are summarized in Table 1.

3. Results and Discussions

3.1. Model Evaluation

Previous studies have evaluated the GC-YIBs model at coarser resolution with global observations and showed that the coupling of GEOS-Chem with YIBs improves the temporal variability of V_{d,O_3} (Lei et al., 2020). Here, we continue to evaluate the performance of nested GC-YIBs over Asia with fine resolution of 0.5° latitude × 0.625° longitude. Observed ozone fluxes at four sites in China, Thailand and Borneo are used to evaluate simulated V_{d,O_3} (Table S3). Both the GEOS-Chem and the GC-YIBs capture the magnitude of monthly mean V_{d,O_3} with biases ranging from −0.12 to +0.13 cm s^{-1}. GC-YIBs shows better performance than GEOS-Chem in most sites (Table S3). Especially, GC-YIBs is able to capture the variations in V_{d,O_3} between dry and wet season. However, observational sites with V_{d,O_3} are quite sparse over Asia (Clifton et al., 2020), limiting our evaluation of V_{d,O_3} at the regional scale. As an alternative, we assess the simulated O_3 concentrations with the updated vegetation processes.

Figure S3 compares the simulated seasonal-mean V_{d,O_3} between GC and GC-YIBs model. The coupling of GC-YIBs increases V_{d,O_3} over China compared to the GEOS-Chem model (Figure S3c). Following such changes, correlation coefficients and normalized mean biases (NMBs) between observed and simulated MDA8 O_3 concentrations at individual sites are improved in GC-YIBs. The correlation coefficients show a widespread increase (Figure S3f). Averaged over the 717 sites in the whole China, the NMB is reduced from 21.4% in GEOS-Chem to 17.9% in GC-YIBs (Figure S3i). It suggests that the increased V_{d,O_3} as a result of dynamically updating YIBs LAI and stomatal conductance in Wesely (1989) scheme alleviates the overestimates of seasonal-mean MDA8 O_3 concentrations in GEOS-Chem.

We further evaluate the daily time series of MDA8 O_3 concentrations over North China and YRD (Figure S4). The correlation coefficient between the observed and simulated regional mean daily MDA8 O_3 concentrations by GC-YIBs is 0.83 in North China and 0.80 in YRD, indicating GC-YIBs model is able to capture daily variations of O_3. The O_3 levels during OPEs are underestimated with NMB of −17.4% in North China and −14.6% in YRD. The difficulty of capturing peak O_3 concentrations during OPEs is a common issue in current air quality models including the GEOS-Chem model (Gong & Liao, 2019; Ni et al., 2018; Zhang & Wang, 2016), WRF-Chem (Tie et al., 2009), and WRF-CMAQ model (Shu et al., 2016).

3.2. Contributions of Enhanced BVOCs and Reduced V_{d,O_3} to OPEs

The 10 OPEs in North China and 5 OPEs in YRD from EX_GC-YIBs experiment are composited first to examine the differences in environmental conditions, such as daily maximum 2-m temperature (Tmax), daily mean relative humidity (RH), BVOC emissions and V_{d,O_3}, between OPE periods and seasonal mean (Figures S5 and S6). With high temperature during OPEs, BVOC emissions increase, respectively, 2.6×10^{-6} kg C m^{-2} day^{-1} (60.5%) and 8.0×10^{-6} kg C m^{-2} day^{-1} (90.0%) over North China and YRD compared to seasonal-mean; while the dry weather leads to reductions in stomatal conductance of vegetation and thus weakens O_3 sinks (reducing dry deposition velocity by 0.013 (5.2%) in North China and by 0.041 cm s^{-1} (14.2%) in YRD compared to seasonal mean). These two processes further enhance O_3 levels during OPEs.

By performing the sensitivity experiments as described in Section 2.3, we first defined the differences in MDA8 O_3 concentrations in EX_GC-YIBs between OPEs and seasonal-mean as the O_3 enhancements during OPEs, which can be further divided into vegetation contributions (including the impacts of increased BVOCs or reduced V_{d,O_3} during OPEs) and nonvegetation contributions (the residual part, indicating processes such as increases in chemical reaction rates, (Fu et al., 2015; Gong & Liao, 2019) and regional transports (Gong et al., 2020b; Han et al., 2018)). Figure S7 shows that the averages of simulated MDA8 O_3 enhancements during OPEs are 16.7 and 16.6 ppbv in North China and YRD, respectively, of which the increases in BVOCs on average promote MDA8 O_3 concentrations during OPEs by 0.45 ppbv (2.7% of the O_3 enhancement) in North China (EX_GC-YIBs minus CASE_BVOCs-fixed-NC) and 2.4 ppbv (14.5% of the O_3 enhancement) in YRD (EX_GC-YIBs minus CASE_BVOCs-fixed-YRD). Such increases in O_3 caused by changes in BVOC emissions can reach as high as 4.7 ppbv (OPE #8 in Table S1 and 28.1% of the O_3 enhancement) in North China and 7.6 ppbv (OPE #5 in Table S1 and 45.8% of the O_3 enhancement) in YRD.

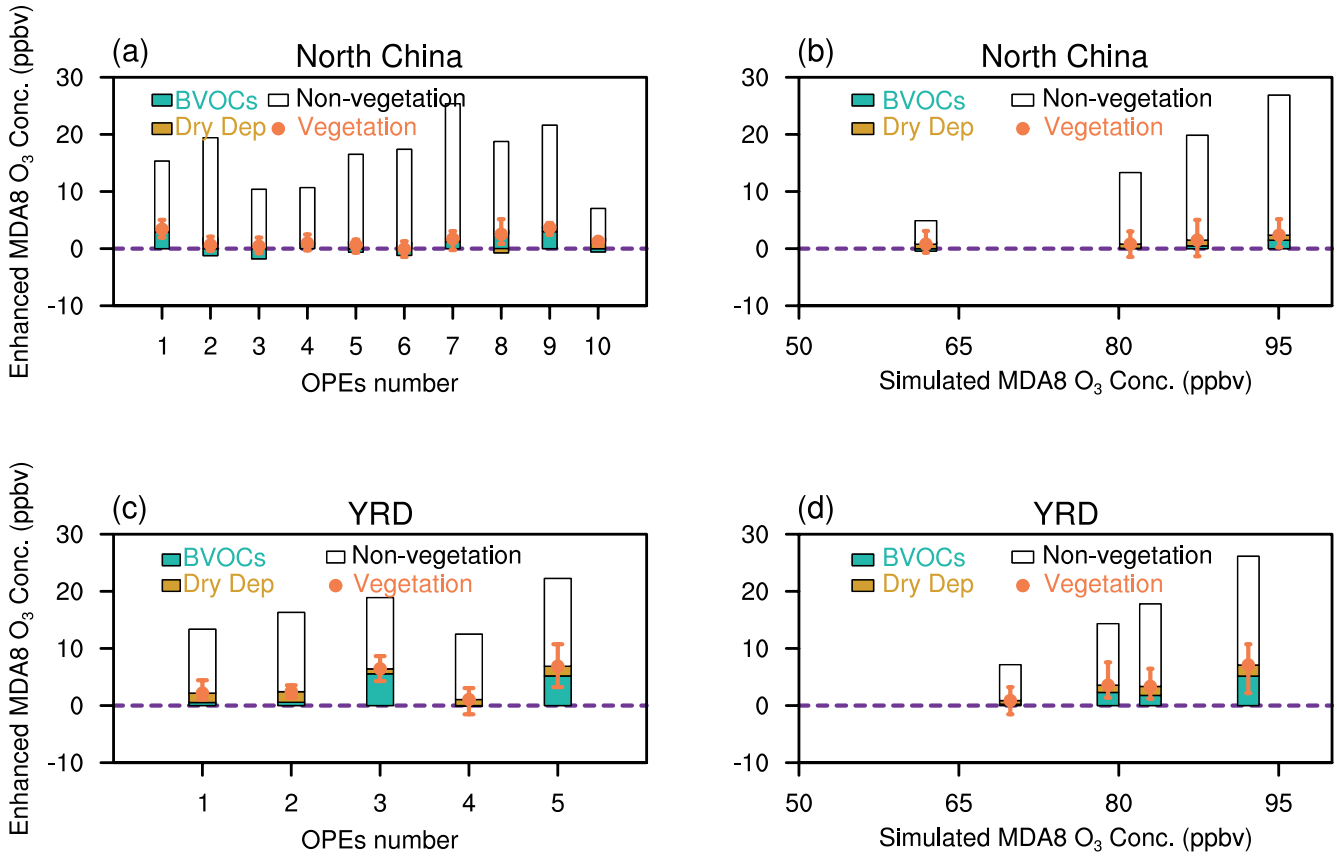

Figure 2. Contributions of vegetation (enhanced BVOC emissions and reduced stomatal dry deposition) and nonvegetation processes during OPEs. Nonvegetation contributions are defined as the residue subtracting vegetation contributions from the simulated total MDA8 O_3 enhancements during OPEs. (a) and (c) shows the averaged vegetation and nonvegetation contributions over each OPE in North China and YRD, respectively. The OPE numbers are following Table S1. (b) and (d) sorts all days during OPEs by simulated MDA8 O_3 concentrations in each region and then equally divides them into four bins. Contributions under different MDA8 O_3 levels are exhibited. The uncertainty bars include all of the daily vegetation contributions at each OPE or bin. VOC, volatile organic compounds; BVOC, biogenic VOC; OPEs, ozone pollution episodes; MDA8, maximum daily 8-h average; YRD, Yangtze River Delta.

Reduced dry deposition on average promotes 0.95 ppbv (5.7% of the O_3 enhancement, EX_GC-YIBs minus CASE_Vd-fixed-NC) and 1.4 ppbv (8.4% of the O_3 enhancement, EX_GC-YIBs minus CASE_Vd-fixed-YRD) in these two regions. Overall, the joint vegetation processes increase MDA8 O_3 during OPEs by 1.4 ppbv (8.4% of the O_3 enhancement) in North China and 3.8 ppbv in YRD (22.9% of the O_3 enhancement). The higher values in YRD than in North China can be attributed to the higher forest coverage in that region (Figure S2).

Figure 2 further shows vegetation and nonvegetation contributions for each OPE (Figures 2a and 2c) as well as under different O_3 pollution levels (Figures 2b and 2d). In North China, vegetation contributes little (0.8–2.4 ppbv) to ambient O_3 concentrations (Figure 2b). In YRD region, vegetation-induced O_3 enhancement varies from 0.9 ppbv (12.5% of the averaged O_3 enhancement of 7.2 ppbv) in slightly polluted days (MDA8 O_3 concentrations at the first quartile of OPEs) to 7.1 ppbv (27.0% of the O_3 enhancement 26.3 ppbv) in the most polluted days (MDA8 O_3 concentrations at the last quartile of OPEs) (Figure 2d). It further suggests that vegetation-induced O_3 enhancement during OPEs is larger in YRD region than in North China.

3.3. Feedback to Surface O_3 Caused by O_3 Damages to Vegetation

Figure 3 shows differences in MDA8 O_3 concentrations between EX_GC-YIBs-damage and EX_GC-YIBs experiments, which represent the feedback of O_3 vegetation damages onto surface O_3 concentrations. The feedback is positive because O_3 inhibits plant stomatal conductance and consequently reduces O_3 dry deposition (Gong et al., 2020a; Sadiq et al., 2017). As a result, seasonal-mean enhancement in MDA8 O_3

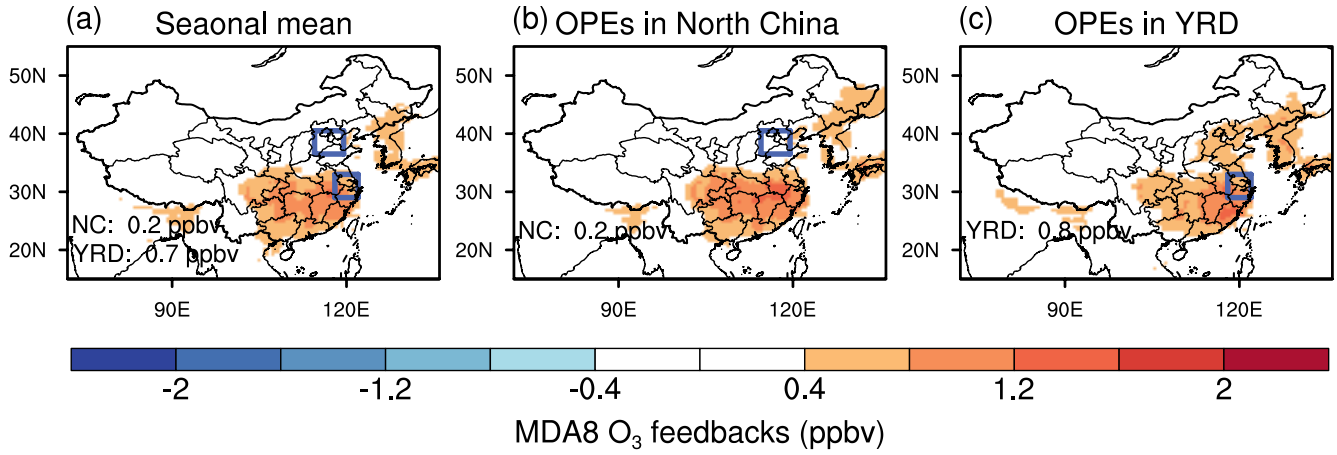

Figure 3. The feedbacks onto MDA8 O_3 concentrations induced by O_3 damage effects to vegetation (a) averaged over May to October in 2014–2017 and during OPEs in (b) North China and (c) YRD regions. The regionally averaged values over North China (NC) and YRD are given in the left corner, respectively. The blue lines enclose North China and YRD, respectively. MDA8, maximum daily 8-h average; OPEs, ozone pollution episodes; YRD, Yangtze River Delta.

concentrations was 0.2 ppbv (0.3% relative to seasonal mean) in North China and 0.7 ppbv (1.1% relative to seasonal mean) in YRD region (Figure 3a). However, such enhancement does not exacerbate during OPEs (Figures 3b and 3c) despite the higher O_3 concentrations during OPEs.

We further explore the relationships among MDA8 O_3 concentrations, RH, and the O_3 enhancement induced by O_3 vegetation damages (Figure s8). Strong feedbacks generally occur in days with moderate to high O_3 levels and wet conditions (RH exceeding 60%) in both North China and YRD. Dry weather favors the occurrence of OPEs (Gong & Liao, 2019; Liu et al., 2019), but meanwhile increases water stress and stimulates vegetation to close stomata to prevent water loss (Li et al., 2019; Matyssek et al., 2006). The reduced stomatal conductance leads to lower stomatal O_3 uptake, buffering the damages from increased O_3. As a result, the feedback induced by O_3 vegetation damages has limited contributions to the O_3 enhancements during OPEs.

In summary, we applied a newly developed chemistry-biosphere coupled model (GC-YIBs) to quantify the contributions of changes in BVOC emissions and stomatal dry deposition in the presence/absence of O_3 vegetation damages to the O_3 enhancements during OPEs over May to October of 2014–2017 in North China and YRD. Compared to the seasonal mean, the increased BVOC emissions by high temperature and reduced V_{d,O_3} by low RH during OPEs together enhanced MDA8 O_3 concentrations by 1.4 ppbv in North China and 3.8 ppbv in YRD. The maximum total contributions at some specific days could exceed 10 ppbv. The O_3 damages to photosynthesis and stomata on average led to an increase in MDA8 O_3 of 0.2 ppbv in North China and of 0.7 ppbv in YRD, but such increases were not exacerbated during OPEs because the reduced stomatal conductance under dry weather inhibits O_3 uptake and thus buffers the high O_3 damages. Our results highlight the important contributions of vegetation processes to the persistent OPEs in eastern China.

Our simulated vegetation contributions to OPEs show comparable magnitude as other processes, especially for the YRD region with high vegetation cover. For instance, regional O_3 transports were reported to contribute about 36% of O_3 enhancement during OPEs in North China (Gong et al., 2020b), while results from this work show that vegetation processes account for 8.4% of O_3 enhancement during OPEs in North China and 22.9% of that in YRD (Figures 2 and S7). Furthermore, reduced stomatal dry deposition was found to promote MDA8 O_3 up to 8 ppbv in Europe during extremely drought events (Lin et al., 2020). It should be noted that the vegetation contributions to OPEs may still be underestimated in our study, because some positive feedbacks (e.g., the increased leaf temperature by closed stomata, Gong et al., 2020a; Sadiq et al., 2017, and the enhanced isoprene from water stress, Zhang & Wang, 2016) are not considered.

Although the influences of BVOCs emissions (e.g., Liu et al., 2018; Lu et al., 2019) and stomatal O_3 uptakes (e.g., Kavassalis & Murphy, 2017; Lin et al., 2020; Silva & Heald, 2018) on ground-level O_3 concentrations

were examined separately by previous studies, few studies investigated the two effects together and considered the feedbacks induced by O_3 vegetation damages, especially for the OPEs under extreme weather conditions such as heat waves and drought. For O_3 pollution in China, there existed studies that investigated the impact of vegetation on O_3 by enhanced BVOC emissions at warm temperatures for limited episodes (e.g., Lyu et al., 2019; Ma et al., 2019; Pu et al., 2017). We present, to our knowledge, the first study to comprehensively examine the vegetation contributions, including processes of BVOCs emissions and stomatal O_3 dry depositions, to OPEs by compositing all episodes during warm season.

Our study suggests that about 1/4 of O_3 enhancement during OPEs in YRD is related to vegetation processes. As a result, strong reductions in anthropogenic VOCs are required to offset the contributions led by increased BVOCs during OPEs, especially in regions with high vegetation cover. Furthermore, continuous and valid O_3 dry deposition observations would be urgent and necessary in China to further calibrate the vegetation contributions during OPEs.

Conflict of Interest

The authors declare no conflicts of interest relevant to this study.

Data Availability Statement

Observed O_3 concentrations are obtained from China Ministry of Ecology and Environment (http://datacenter.mee.gov.cn/). Multiresolution Emission Inventory for China can be accessed publicly from http://meicmodel.org/. The model output used in this study can be accessed via https://zenodo.org/record/4471200#.YGKVfa8zZPY.

Acknowledgments
This work was jointly supported by the National Natural Science Foundation of China (Grant No. 42021004) and the National Key Research and Development Program of China (Grant No. 2019YFA0606800).

References

Ainsworth, E. A., Yendrek, C. R., Sitch, S., Collins, W. J., & Emberson, L. D. (2012). The effects of tropospheric ozone on net primary productivity and implications for climate change. *Annual Review of Plant Biology*, *63*, 637–661. https://doi.org/10.1146/annurev-arplant-042110-103829

Atkinson, R. (2000). Atmospheric chemistry of VOCs and NOx. *Atmospheric Environment*, *34*(12–14), 2063–2101. https://doi.org/10.1016/s1352-2310(99)00460-4

Ball, J. T., Woodrow, I. E., & Berry, J. A. (1987). A model predicting stomatal conductance and its contribution to the control of photosynthesis under different environmental conditions. *Progress in Photosynthesis Research*, *4*, 221–224. https://doi.org/10.1007/978-94-017-0519-6_48

Bey, I., Jacob, D. J., Yantosca, R. M., Logan, J. A., Field, B. D., Fiore, A. M., et al. (2001). Global modeling of tropospheric chemistry with assimilated meteorology: Model description and evaluation. *Journal of Geophysical Research*, *106*(D19), 23073–23095. https://doi.org/10.1029/2001JD000807

Bian, H. S., & Prather, M. J. (2002). Fast-J2: Accurate simulation of stratospheric photolysis in global chemical models. *Journal of Atmospheric Chemistry*, *41*(3), 281–296. https://doi.org/10.1023/a:1014980619462

Calfapietra, C., Fares, S., Manes, F., Morani, A., Sgrigna, G., & Loreto, F. (2013). Role of biogenic volatile organic compounds (BVOC) emitted by urban trees on ozone concentration in cities: A review. *Environmental Pollution*, *183*, 71–80. https://doi.org/10.1016/j.envpol.2013.03.012

Chen, K., Wang, P., Zhao, H., Wang, P., Gao, A., Myllyvirta, L., & Zhang, H. (2021). Summertime O-3 and related health risks in the north China plain: A modeling study using two anthropogenic emission inventories. *Atmospheric Environment*, *246*, 118087. https://doi.org/10.1016/j.atmosenv.2020.118087

Clifton, O. E., Fiore, A. M., Massman, W. J., Baublitz, C. B., Coyle, M., Emberson, L., et al. (2020). Dry deposition of ozone over land: Processes, measurement, and modeling. *Reviews of Geophysics*, *58*, e2019RG000670. https://doi.org/10.1029/2019RG000670

Dang, R., & Liao, H. (2019). Radiative forcing and health impact of aerosols and ozone in China as the consequence of clean air actions over 2012–2017. *Geophysical Research Letters*, *46*(21), 12511–12519. https://doi.org/10.1029/2019GL084605

Dang, R., Liao, H., & Fu, Y. (2021). Quantifying the anthropogenic and meteorological influences on summertime surface ozone in China over 2012–2017. *Science of the Total Environment*, *754*, 142394. https://doi.org/10.1016/j.scitotenv.2020.142394

Emberson, L. D., Kitwiroon, N., Beevers, S., Bueker, P., & Cinderby, S. (2013). Scorched Earth: How will changes in the strength of the vegetation sink to ozone deposition affect human health and ecosystems? *Atmospheric Chemistry and Physics*, *13*(14), 6741–6755. https://doi.org/10.5194/acp-13-6741-2013

Fares, S., Oksanen, E., Lannenpaa, M., Julkunen-Tiitto, R., & Loreto, F. (2010). Volatile emissions and phenolic compound concentrations along a vertical profile of Populus nigra leaves exposed to realistic ozone concentrations. *Photosynthesis Research*, *104*(1), 61–74. https://doi.org/10.1007/s11120-010-9549-5

Farquhar, G. D., Caemmerer, S. V., & Berry, J. A. (1980). A biochemical-model of photosynthetic CO_2 assimilation in leaves of C-3 species. *Planta*, *149*(1), 78–90. https://doi.org/10.1007/BFf00386231

Feng, Z., Shang, B., Gao, F., & Calatayud, V. (2019a). Current ambient and elevated ozone effects on poplar: A global meta-analysis and response relationships. *Science of the Total Environment*, *654*, 832–840. https://doi.org/10.1016/j.scitotenv.2018.11.179

Feng, Z., Yuan, X., Fares, S., Loreto, F., Li, P., Hoshika, Y., & Paoletti, E. (2019b). Isoprene is more affected by climate drivers than monoterpenes: A meta-analytic review on plant isoprenoid emissions. *Plant, Cell and Environment*, *42*(6), 1939–1949. https://doi.org/10.1111/pce.13535

Fowler, D., Pilegaard, K., Sutton, M. A., Ambus, P., Raivonen, M., Duyzer, J., et al. (2009). Atmospheric composition change: Ecosystems-atmosphere interactions. *Atmospheric Environment*, *43*(33), 5193–5267.
Fu, T.-M., Zheng, Y., Paulot, F., Mao, J., & Yantosca, R. M. (2015). Positive but variable sensitivity of August surface ozone to large-scale warming in the southeast United States. *Nature Climate Change*, *5*(5), 454–458. https://doi.org/10.1038/nclimate2567
Fuhrer, J., Skarby, L., & Ashmore, M. R. (1997). Critical levels for ozone effects on vegetation in Europe. *Environmental Pollution*, *97*(1–2), 91–106. https://doi.org/10.1016/s0269-7491(97)00067-5
Gong, C., Lei, Y., Ma, Y., Yue, X., & Liao, H. (2020a). Ozone-vegetation feedback through dry deposition and isoprene emissions in a global chemistry-carbon-climate model. *Atmospheric Chemistry and Physics*, *20*(6), 3841–3857. https://doi.org/10.5194/acp-20-3841-2020
Gong, C., & Liao, H. (2019). A typical weather pattern for ozone pollution events in North China. *Atmospheric Chemistry and Physics*, *19*(22), 13725–13740. https://doi.org/10.5194/acp-19-13725-2019
Gong, C., Liao, H., Zhang, L., Yue, X., Dang, R., & Yang, Y. (2020b). Persistent ozone pollution episodes in North China exacerbated by regional transport. *Environmental Pollution* (Barking, Essex: 1987), *265*(Pt A), 115056. https://doi.org/10.1016/j.envpol.2020.115056
Guenther, A. B., Jiang, X., Heald, C. L., Sakulyanontvittaya, T., Duhl, T., Emmons, L. K., & Wang, X. (2012). The model of emissions of gases and aerosols from nature version 2.1 (MEGAN2.1): An extended and updated framework for modeling biogenic emissions. *Geoscientific Model Development*, *5*(6), 1471–1492. https://doi.org/10.5194/gmd-5-1471-2012
Han, X., Zhu, L., Wang, S., Meng, X., Zhang, M., & Hu, J. (2018). Modeling study of impacts on surface ozone of regional transport and emissions reductions over North China Plain in summer 2015. *Atmospheric Chemistry and Physics*, *18*(16), 12207–12221. https://doi.org/10.5194/acp-18-12207-2018
Huang, L., McDonald-Buller, E. C., McGaughey, G., Kimura, Y., & Allen, D. T. (2016). The impact of drought on ozone dry deposition over eastern Texas. *Atmospheric Environment*, *127*, 176–186. https://doi.org/10.1016/j.atmosenv.2015.12.022
Jacob, D. J., & Winner, D. A. (2009). Effect of climate change on air quality. *Atmospheric Environment*, *43*(1), 51–63. https://doi.org/10.1016/j.atmosenv.2008.09.051
Kavassalis, S. C., & Murphy, J. G. (2017). Understanding ozone-meteorology correlations: A role for dry deposition. *Geophysical Research Letters*, *44*(6), 2922–2931. https://doi.org/10.1002/2016GL071791
Kuerban, M., Waili, Y., Fan, F., Liu, Y., Qin, W., Dore, A. J., et al. (2020). Spatio-temporal patterns of air pollution in China from 2015 to 2018 and implications for health risks. *Environmental Pollution*, *258*, 113659. https://doi.org/10.1016/j.envpol.2019.113659
Lei, Y., Yue, X., Liao, H., Gong, C., & Zhang, L. (2020). Implementation of Yale Interactive terrestrial Biosphere model v1.0 into GEOS-Chem v12.0.0: A tool for biosphere-chemistry interactions. *Geoscientific Model Development*, *13*(3), 1137–1153. https://doi.org/10.5194/gmd-13-1137-2020
Lelieveld, J., Evans, J. S., Fnais, M., Giannadaki, D., & Pozzer, A. (2015). The contribution of outdoor air pollution sources to premature mortality on a global scale. *Nature*, *525*(7569), 367–371. https://doi.org/10.1038/nature15371
Liao, Z., Gao, M., Sun, J., & Fan, S. (2017). The impact of synoptic circulation on air quality and pollution-related human health in the Yangtze River Delta region. *Science of the Total Environment*, *607–608*, 838–846. https://doi.org/10.1016/j.scitotenv.2017.07.031
Li, K., Jacob, D. J., Liao, H., Shen, L., Zhang, Q., & Bates, K. H. (2019). Anthropogenic drivers of 2013–2017 trends in summer surface ozone in China. *Proceedings of the National Academy of Sciences of the United States of America*, *116*(2), 422–427. https://doi.org/10.1073/pnas.1812168116
Li, M., Zhang, Q., Kurokawa, J.-i., Woo, J.-H., He, K., Lu, Z., et al. (2017). MIX: A mosaic Asian anthropogenic emission inventory under the international collaboration framework of the MICS-Asia and HTAP. *Atmospheric Chemistry and Physics*, *17*(2), 935–963. https://doi.org/10.5194/acp-17-935-2017
Li, P., Zhou, H., Xu, Y., Shang, B., & Feng, Z. (2019). The effects of elevated ozone on the accumulation and allocation of poplar biomass depend strongly on water and nitrogen availability. *Science of the Total Environment*, *665*, 929–936. https://doi.org/10.1016/j.scitotenv.2019.02.182
Lin, M., Horowitz, L. W., Xie, Y., Paulot, F., Malyshev, S., Shevliakova, E., et al. (2020). Vegetation feedbacks during drought exacerbate ozone air pollution extremes in Europe. *Nature Climate Change*, *10*(5), 444–451. https://doi.org/10.1038/s41558-020-0743-y
Liu, J., Wang, L., Li, M., Liao, Z., Sun, Y., Song, T., et al. (2019). Quantifying the impact of synoptic circulation patterns on ozone variability in northern China from April to October 2013-2017. *Atmospheric Chemistry and Physics*, *19*(23), 14477–14492. https://doi.org/10.5194/acp-19-14477-2019
Liu, Y., Li, L., An, J., Huang, L., Yan, R., Huang, C., et al. (2018). Estimation of biogenic VOC emissions and its impact on ozone formation over the Yangtze River Delta region, China. *Atmospheric Environment*, *186*, 113–128. https://doi.org/10.1016/j.atmosenv.2018.05.027
Liu, Y., & Wang, T. (2020a). Worsening urban ozone pollution in China from 2013 to 2017-Part 2: The effects of emission changes and implications for multi-pollutant control. *Atmospheric Chemistry and Physics*, *20*(11), 6323–6337. https://doi.org/10.5194/acp-20-6323-2020
Liu, Y., & Wang, T. (2020b). Worsening urban ozone pollution in China from 2013 to 2017-Part 1: The complex and varying roles of meteorology. *Atmospheric Chemistry and Physics*, *20*(11), 6305–6321. https://doi.org/10.5194/acp-20-6305-2020
Lombardozzi, D., Levis, S., Bonan, G., & Sparks, J. P. (2012). Predicting photosynthesis and transpiration responses to ozone: Decoupling modeled photosynthesis and stomatal conductance. *Biogeosciences*, *9*(8), 3113–3130. https://doi.org/10.5194/bg-9-3113-2012
Lu, X., Hong, J., Zhang, L., Cooper, O. R., Schultz, M. G., Xu, X., et al. (2018). Severe surface ozone pollution in China: A global perspective. *Environmental Science and Technology Letters*, *5*(8), 487–494. https://doi.org/10.1021/acs.estlett.8b00366
Lu, X., Zhang, L., Chen, Y., Zhou, M., Zheng, B., Li, K., et al. (2019). Exploring 2016–2017 surface ozone pollution over China: Source contributions and meteorological influences. *Atmospheric Chemistry and Physics*, *19*(12), 8339–8361. https://doi.org/10.5194/acp-19-8339-2019
Lu, X., Zhang, L., Wang, X., Gao, M., Li, K., Zhang, Y., et al. (2020). Rapid increases in warm-season surface ozone and resulting health impact in China since 2013. *Environmental Science and Technology Letters*, *7*(4), 240–247. https://doi.org/10.1021/acs.estlett.0c00171
Lyu, X., Wang, N., Guo, H., Xue, L., Jiang, F., Zeren, Y., et al. (2019). Causes of a continuous summertime O-3 pollution event in Jinan, a central city in the North China Plain. *Atmospheric Chemistry and Physics*, *19*(5), 3025–3042. https://doi.org/10.5194/acp-19-3025-2019
Ma, M., Gao, Y., Wang, Y., Zhang, S., Leung, L. R., Liu, C., et al. (2019). Substantial ozone enhancement over the North China Plain from increased biogenic emissions due to heat waves and land cover in summer 2017. *Atmospheric Chemistry and Physics*, *19*(19), 12195–12207. https://doi.org/10.5194/acp-19-12195-2019
Matyssek, R., Le Thiec, D., Low, M., Dizengremel, P., Nunn, A. J., & Haberle, K. H. (2006). Interactions between drought and O-3 stress in forest trees. *Plant Biology*, *8*(1), 11–17. https://doi.org/10.1055/s-2005-873025
Molod, A., Takacs, L., Suarez, M., & Bacmeister, J. (2015). Development of the GEOS-5 atmospheric general circulation model: Evolution from MERRA to MERRA2. *Geoscientific Model Development*, *8*(5), 1339–1356. https://doi.org/10.5194/gmd-8-1339-2015

Ni, R., Lin, J., Yan, Y., & Lin, W. (2018). Foreign and domestic contributions to springtime ozone over China. *Atmospheric Chemistry and Physics*, *18*(15), 11447–11469. https://doi.org/10.5194/acp-18-11447-2018

Olson, D. M., Dinerstein, E., Wikramanayake, E. D., Burgess, N. D., Powell, G. V. N., Underwood, E. C., et al. (2001). Terrestrial ecoregions of the worlds: A new map of life on Earth. *BioScience*, *51*(11), 933–938. https://doi.org/10.1641/0006-3568(2001)051[0933:TEOTWA]2.0.CO;2

Park, R. J., Jacob, D. J., Chin, M., & Martin, R. V. (2003). Sources of carbonaceous aerosols over the United States and implications for natural visibility. *Journal of Geophysical Research*, *108*(D12), 4355. https://doi.org/10.1029/2002JD003190

Porter, W. C., & Heald, C. L. (2019). The mechanisms and meteorological drivers of the summertime ozone-temperature relationship. *Atmospheric Chemistry and Physics*, *19*(21), 13367–13381. https://doi.org/10.5194/acp-19-13367-2019

Pu, X., Wang, T. J., Huang, X., Melas, D., Zanis, P., Papanastasiou, D. K., & Poupkou, A. (2017). Enhanced surface ozone during the heat wave of 2013 in Yangtze River Delta region, China. *Science of the Total Environment*, *603–604*, 807–816. https://doi.org/10.1016/j.scitotenv.2017.03.056

Pusede, S. E., Steiner, A. L., & Cohen, R. C. (2015). Temperature and recent trends in the chemistry of continental surface ozone. *Chemistry Review*, *115*(10), 3898–3918. https://doi.org/10.1021/cr5006815

Pye, H. O. T., Liao, H., Wu, S., Mickley, L. J., Jacob, D. J., Henze, D. K., & Seinfeld, J. H. (2009). Effect of changes in climate and emissions on future sulphate-nitrate-ammonium aerosol levels in the United States. *Journal of Geophysical Research 114*, D01205. https://doi.org/10.1029/2008JD010701

Sadiq, M., Tai, A. P. K., Lombardozzi, D., & Martin, M. V. (2017). Effects of ozone-vegetation coupling on surface ozone air quality via biogeochemical and meteorological feedbacks. *Atmospheric Chemistry and Physics*, *17*(4), 3055–3066. https://doi.org/10.5194/acp-17-3055-2017

Shu, L., Xie, M., Wang, T., Gao, D., Chen, P., Han, Y., et al. (2016). Integrated studies of a regional ozone pollution synthetically affected by subtropical high and typhoon system in the Yangtze River Delta region, China. *Atmospheric Chemistry and Physics*, *16*(24), 15801–15819. https://doi.org/10.5194/acp-16-15801-2016

Sillman, S. (1999). The relation between ozone, NOx and hydrocarbons in urban and polluted rural environments. *Atmospheric Environment*, *33*(12), 1821–1845. https://doi.org/10.1016/s1352-2310(98)00345-8

Silva, S. J., & Heald, C. L. (2018). Investigating dry deposition of ozone to vegetation. *Journal of Geophysical Research: Atmospheres*, *123*, 559–573. https://doi.org/10.1002/2017JD027278

Sitch, S., Cox, P. M., Collins, W. J., & Huntingford, C. (2007). Indirect radiative forcing of climate change through ozone effects on the land-carbon sink. *Nature*, *448*(7155), 791–794. https://doi.org/10.1038/nature06059

Tie, X., Geng, F., Peng, L., Gao, W., & Zhao, C. (2009). Measurement and modeling of O-3 variability in Shanghai, China: Application of the WRF-Chem model. *Atmospheric Environment*, *43*(28), 4289–4302. https://doi.org/10.1016/j.atmosenv.2009.06.008

Val Martin, M., Heald, C. L., & Arnold, S. R. (2014). Coupling dry deposition to vegetation phenology in the Community Earth SystemModel: Implications for the simulation of surface O3. *Geophysical Research Letters*, *41*, 2988–2996. https://doi.org/10.1002/2014GL059651

Velikova, V., Fares, S., & Loreto, F. (2008). Isoprene and nitric oxide reduce damages in leaves exposed to oxidative stress. *Plant, Cell and Environment*, *31*(12), 1882–1894. https://doi.org/10.1111/j.1365-3040.2008.01893.x

Wang, N., Lyu, X. P., Deng, X. J., Huang, X., Jiang, F., & Ding, A. J. (2019). Aggravating O-3 pollution due to NOx emission control in eastern China. *Science of the Total Environment*, *677*, 732–744. https://doi.org/10.1016/j.scitotenv.2019.04.388

Wang, T., Xue, L., Brimblecombe, P., Lam, Y. F., Li, L., & Zhang, L. (2017). Ozone pollution in China: A review of concentrations, meteorological influences, chemical precursors, and effects. *Science of the Total Environment*, *575*, 1582–1596. https://doi.org/10.1016/j.scitotenv.2016.10.081

Wang, Y., Zhang, Y., Hao, J., & Luo, M. (2011). Seasonal and spatial variability of surface ozone over China: Contributions from background and domestic pollution. *Atmospheric Chemistry and Physics*, *11*(7), 3511–3525. https://doi.org/10.5194/acp-11-3511-2011

Wang, Y. T., Zhao, Y., Zhang, L., Zhang, J., & Liu, Y. (2020). Modified regional biogenic VOC emissions with actual ozone stress and integrated land cover information: A case study in Yangtze River Delta, China. *Science of the Total Environment*. *727*, 138703.

Wesely, M. L. (1989). Parameterization of surface resistances to gaseous dry deposition in regional-scale numerical-models. *Atmospheric Environment*, *23*(6), 1293–1304. https://doi.org/10.1016/0004-6981(89)90153-4

Wesely, M. L., & Hicks, B. B. (2000). A review of the current status of knowledge on dry deposition. *Atmospheric Environment*, *34*(12–14), 2261–2282. https://doi.org/10.1016/s1352-2310(99)00467-7

Wittig, V. E., Ainsworth, E. A., & Long, S. P. (2007). To what extent do current and projected increases in surface ozone affect photosynthesis and stomatal conductance of trees? A meta-analytic review of the last 3 decades of experiments. *Plant, Cell and Environment*, *30*(9), 1150–1162. https://doi.org/10.1111/j.1365-3040.2007.01717.x

Yuan, X., Feng, Z., Liu, S., Shang, B., Li, P., Xu, Y., & Paoletti, E. (2017). Concentration-and flux-based dose-responses of isoprene emission from poplar leaves and plants exposed to an ozone concentration gradient. *Plant, Cell and Environment*, *40*(9), 1960–1971. https://doi.org/10.1111/pce.13007

Yue, X., & Unger, N. (2014). Ozone vegetation damage effects on gross primary productivity in the United States. *Atmospheric Chemistry and Physics*, *14*(17), 9137–9153. https://doi.org/10.5194/acp-14-9137-2014

Yue, X., & Unger, N. (2015). The Yale interactive terrestrial Biosphere model version 1.0: Description, evaluation and implementation into NASA GISS ModelE2, *Geoscientific Model Development*, *8*(8), 2399–2417. https://doi.org/10.5194/gmd-8-2399-2015

Yue, X., Unger, N., Harper, K., Xia, X., Liao, H., Zhu, T., et al. (2017). Ozone and haze pollution weakens net primary productivity in China. *Atmospheric Chemistry and Physics*, *17*(9), 6073–6089. https://doi.org/10.5194/acp-17-6073-2017

Zhang, Y., & Wang, Y. (2016). Climate-driven ground-level ozone extreme in the fall over the Southeast United States. *Proceedings of the National Academy of Sciences of the United States of America*, *113*(36), 10025–10030. https://doi.org/10.1073/pnas.1602563113

Zheng, B., Tong, D., Li, M., Liu, F., Hong, C., Geng, G., et al. (2018). Trends in China's anthropogenic emissions since 2010 as the consequence of clean air actions. *Atmospheric Chemistry and Physics*, *18*(19), 14095–14111. https://doi.org/10.5194/acp-18-14095-2018

References From the Supporting Information

Fowler, D., Nemitz, E., Misztal, P., Marco, C. D., Skiba, U., Ryder, J., et al. (2011). Effects of land use on surface-atmosphere exchanges of trace gases and energy in Borneo: Comparing fluxes over oil palm plantations and a rainforest. *Philosophical Transactions of the Royal Society B: Biological Sciences*, *366*(1582), 3196–3209.

Matsuda, K., Watanabe, I., & Wingpud, V. (2005). Ozone dry deposition above a tropical forest in the dry season in northern Thailand. *Atmospheric Environment*, *39*(14), 2571–2577.

Matsuda, K., Watanabe, I., Wingpud, V., Theramongkol, P., & Ohizumi, T. (2006). Deposition velocity of O-3 and SO_2 in the dry and wet season above a tropical forest in northern Thailand. *Atmospheric Environment*, *40*(39), 7557–7564.

Sorimachi, A., Sakamoto, K., Ishihara, H., Fukuyama, T., Utiyama, M., Wang, W., et al. (2003). Measurements of sulfur dioxide and ozone dry deposition over short vegetation in northern China - A preliminary study. *Atmospheric Environment*, *37*(22), 3157–3166.

Zhu, Z. L., Sun, X. M., Dong, Y. S., Zhao, F. H., & Meixner, F. X. (2014). Diurnal variation of ozone flux over corn field in Northwestern Shandong Plain of China. *Science China Earth Sciences*, *57*(3), 503–511.